Extreme Heat and Rainfall Risk Attributed to Cumulative CO_2 Emissions from Fossil Fuel Producers

Christopher W. Callahan[1]

[1]O'Neill School of Public and Environmental Affairs, Indiana University, Bloomington, IN, USA

Corresponding author: Christopher Callahan (ccallah@iu.edu)

Key Points:

- Extreme heat and rainfall risk are modeled as functions of cumulative CO_2 emissions.
- Individual emitters have contributed to extreme heat and rainfall risk due to their contributions to historical cumulative CO_2 emissions.
- This framework can be applied to any emitter to facilitate efficient climate liability assessments.

Abstract

Legal and political approaches to climate accountability require demonstrating that a particular emitter contributed to a climate impact, but quantitative solutions to this attribution challenge remain nascent. This study leverages the proportionality of global warming to cumulative CO_2 emissions to develop statistical models that directly predict extreme climate risk from cumulative emissions. Results show that cumulative emissions from individual actors have increased the probability of extreme heat and rainfall globally; for example, emissions from the United States have increased the risk of recent extreme heat by at least 50% for one-third of the globe. Focusing on specific events demonstrates that emissions from major fossil fuel firms increased the likelihood of the 2021 Pacific Northwest heat wave by 31% and 2022 extreme rainfall in Pakistan by 7%. These results demonstrate a flexible attribution framework grounded in the proportional relationships that inform climate policy, with the potential to guide efficient climate accountability assessments.

Plain Language Summary

It is difficult to determine which fossil fuel emitter contributed to an extreme climate event like a heat wave or a flood. To help close this gap, this paper shows that there is a direct proportionality between cumulative carbon dioxide emissions and the probability of extreme heat and rainfall. As a result, given the contributions that major countries and fossil fuel producers have made to historical emissions, their contributions to the increasing risk of extreme heat and rainfall can be directly inferred. This approach can be flexibly applied to many types of emitters and extreme events at any location or time; for example, it can be used to show that emissions from ExxonMobil, Chevron, and other major fossil fuel producers increased the risk of extreme heat in the Pacific Northwest. This framework has the potential to inform future assessments of the liability of major emitters for extreme heat and rainfall.

1 Introduction

As the human toll of greenhouse gas (GHG) emissions accumulates, recent legal and political efforts have demanded accountability for climate change. Lawsuits against fossil fuel producers over climate damages have proliferated (Setzer & Higham, 2024), and multiple U.S. states have passed "polluters pay" laws to recoup the costs of climate adaptation by charging fossil fuel producers (Calhoun et al., 2025). Internationally, climate negotiations have established a financing facility for loss and damage payments (Clarke et al., 2023), and the International Court of Justice recently affirmed the legal obligations of states to mitigate climate change (Phelan et al., 2025).

Each of these approaches to climate accountability either explicitly or implicitly requires connecting an individual emitter to some downstream climate impact. In many jurisdictions, a plaintiff can only sue if they can demonstrate a causal connection between a defendant and a particularized injury. However, because GHGs are long-lived and innumerable actors have emitted, it is difficult to attribute responsibility for any particular climate impact (Kysar, 2011). In the face of this gap, climate change attribution science might provide scientific support for climate accountability by linking an individual climate event or impact to greenhouse gas emissions (Allen, 2003; Burger et al., 2020; Callahan & Mankin, 2025). Indeed, advances in climate modeling and causal inference now make it possible to develop "end-to-end" or "source-to-impact" attribution analyses that link individual emitters to rising global temperature

(Ekwurzel et al., 2017), sea level rise (Sadai et al., 2025), extreme heat events (Beusch et al., 2022; Callahan & Mankin, 2025; Quilcaille et al., 2025), wildfire burned area (Dahl et al., 2023), and the economic damages from climate change (Burke et al., 2026; Callahan & Mankin, 2022, 2025).

At the same time, it is now well-understood that global temperature change is linearly proportional to cumulative CO_2 emissions (IPCC, 2021). Higher emissions cause the radiative forcing effect of CO_2 to saturate, but also cause each pulse of CO_2 to have a higher airborne fraction due to carbon sink weakening; the approximate cancellation of these nonlinearities yields a linear relationship (Matthews et al., 2009). The risk of extreme heat and heavy precipitation has similarly been shown to be proportional to global temperature rise (Fischer & Knutti, 2015; IPCC, 2021; Seneviratne et al., 2016). While these facts are well-known to influence climate policy, including as the scientific basis for "net zero" emissions targets (Matthews & Caldeira, 2008), they also have important implications for questions of causation in climate attribution and accountability. In particular, they imply that the causal chain from emissions to impacts is simple: each additional ton of CO_2 discernibly increases extreme climate risk.

There is, therefore, potential to clarify climate accountability by leveraging these proportional relationships. However, existing end-to-end attribution studies have generally been ad hoc, choosing particular actors of interest such as fossil fuel producers (Callahan & Mankin, 2025; Dahl et al., 2023; Ekwurzel et al., 2017; Quilcaille et al., 2025), countries (Beusch et al., 2022; Callahan & Mankin, 2022; Otto et al., 2017), or individuals (Lott et al., 2021; Schöngart et al., 2025). The community has not yet identified a single unifying framework for end-to-end attribution that can be applied to a wide range of actors without needing to re-run custom model simulations. Furthermore, some studies have made advances by connecting particular actors' emissions to downstream human impacts such as economic losses (Burke et al., 2026; Callahan & Mankin, 2022, 2025) or selected high-impact events from damage databases (Quilcaille et al., 2025). Yet each community's claim for restitution is usually specific to their experience and not necessarily captured by global damage estimates. As a result, it may be productive to establish a generalized framework focused on the risk of physical extreme events rather than attempting to enumerate all the specific human impacts for which attribution can be performed. This is especially true given that probabilistic assessments of risk have been accepted by some previous courts in lieu of specific damage enumerations (Saad, 2023).

This study develops a unifying end-to-end attribution framework by fitting statistical models that directly relate extreme heat and rainfall probability to cumulative CO_2 emissions (Fig. 1, Fig. S1). These estimates can then be applied to any actor whose CO_2 emissions are known without having to re-estimate the key underlying parameters, making the approach efficient and flexible.

Specifically, the framework models annual maximum daily high temperature ("TXx") and annual maximum daily accumulated rainfall ("Rx1day") using nonstationary generalized extreme value (GEV) distributions fitted to large ensembles of climate model simulations (Methods). The GEV location and scale parameters are specified as linear functions of cumulative CO_2 emissions. Nonstationary GEVs are fitted separately to each land grid cell in each of 171 realizations of 8 unique global climate models (GCMs), sampling across many realizations of internal climate variability and multiple model structures. Using the fitted parameters, the risk of extreme events can be predicted in observations as a function of

historically observed emissions, with a focus on the most extreme recent heat and rainfall at each grid cell. Changing extreme event risk globally can then be attributed to individual actors by calculating the probability of extreme events with and without that actor's emissions (Fig. 1).

This approach is inspired by the use of nonstationary GEVs in the extreme event attribution literature (Philip et al., 2020; Risser, Zhang, et al., 2025; Risser & Wehner, 2017). However, this study depart from prior literature by fitting GEVs to GCMs rather than observations, because observations have short records (Zeder et al., 2023) and limited spatial coverage (Diffenbaugh et al., 2017), and can be vulnerable to selection bias on high-impact events (Miralles & Davison, 2023; van Oldenborgh et al., 2021). Instead, the approach uses GCMs as training data for statistical models which are then applied out-of-sample to observed emissions (Trok et al., 2024). Large initial-condition ensembles can be used to estimate reliable statistics for extreme events (Deser et al., 2020; Diffenbaugh et al., 2017) by fitting GEV parameters across thousands of model-years, many realizations of natural variability, and a wide range of cumulative emissions levels. This approach can be seen as a hybrid between experimental and statistical approaches to extreme event attribution (Risser, Ombadi, et al., 2025), leveraging the benefits of GCMs but ultimately applying the results to observationally defined counterfactual emissions and extreme events.

2 Materials and Methods

2.1 Data

This study uses global climate model (GCM) output from the Multi-Model Large Ensemble Archive (MMLEA) version 2 (Maher et al., 2025). This archive combines initial-condition ensembles from multiple climate models from the sixth phase of the Coupled Model Intercomparison Project (CMIP6), yielding 171 individual realizations from 8 unique models that run the historical (1850-2014) and SSP5-8.5 (2015-2100) emissions scenarios (Table S1). The use of SSP5-8.5 comes directly from the MMLEA archive, but it is particularly advantageous here because it provides a wide range of cumulative emissions levels and extreme heat and rainfall magnitudes, enhancing statistical power. The models used here also span a range of Equilibrium Climate Sensitivity values (Meehl et al., 2020), which is helpful in accounting for uncertainty in the sensitivity of the climate to CO_2 emissions.

Temperature data come from the ERA5 renanalysis (Hersbach et al., 2020) and precipitation data come from the CPC interpolated gauge dataset (Xie et al., 2010). ERA5 data are downloaded at the hourly resolution, aggregated to daily maxima, and then aggregated to annual maxima (i.e., TXx). The CPC data are downloaded as daily totals and aggregated to annual maxima (i.e., Rx1day). Both observational datasets are regridded to a 2.5°-by-2.5° resolution to match the MMLEA grid.

Each MMLEA realization is bias-corrected by setting its mean over 1981-2010 to be equal to the observed 1981-2010 mean at each grid cell. This bias correction is helpful to ensure that model-derived parameters do not yield widely varying estimates of the probability of observed extreme events, since models can differ from observed temperatures by multiple degrees in regions such as the Pacific Northwest (Fig. S2).

Observed global emissions over 1750-2023 come from the Global Carbon Budget (Friedlingstein et al., 2025), country-specific emissions over 1750-2022 come from CEDS (Hoesly et al., 2018), and emissions for fossil fuel producers come from the Carbon Majors

database developed by Heede (2014) and now maintained by the nonprofit InfluenceMap. While the Carbon Majors database has different years of data coverage for different firms, cumulative emissions are calculated from the first date available for each firm and stopping in 2020 in each case (Callahan & Mankin, 2025).

The GCMs used in this study are driven by prescribed GHG concentrations rather than being fully coupled to emissions and the carbon cycle. The emissions are derived from Integrated Assessment Models that determine internally consistent emissions trajectories that would produce the end-of-century radiative forcing associated with each climate scenario. This analysis could be performed using emissions-driven Earth system models (ESMs) with coupled carbon cycles, but there are only a small number of those simulations available in comparison to the hundreds of realizations currently available from CMIP6 GCMs. As CMIP7 moves towards prioritizing and standardizing emissions-driven experiments with ESMs, more opportunities to use those resources will become available.

2.2 Statistical models

This study models the changing probability of extreme temperature and precipitation as a function of cumulative CO_2 emissions, taking advantage of nonstationary Generalized Extreme Value (GEV) distributions, a widely used tool for analyzing the risk of extreme events (Coles, 2001; Gilleland & Katz, 2016). Specifically, annual maximum daily high temperature (TXx) and annual maximum daily total rainfall (Rx1day) are modeled using GEV distributions that depend three parameters: location μ, scale σ, and shape ζ. The location parameter represents the typical extreme value, the scale parameter represents variability in extreme values, and the shape parameter represents the thickness of the upper tail of the extreme value distribution. Following previous work (Philip et al., 2020; Risser, Zhang, et al., 2025; Risser & Wehner, 2017), the location and scale are allowed to vary over time and the shape is held constant.

The location (μ_t) and scale (σ_t) in each year t are modeled as a function of cumulative CO_2 emissions (E) up through that year:

$$\mu_t = \beta_0 + \beta_1 \sum_{y=1750}^{y=t} E_y$$

$$\sigma_t = \theta_0 + \theta_1 \sum_{y=1750}^{y=t} E_y$$

$$\zeta_t = \zeta$$

At each grid cell, a separate GEV is estimated for each GCM realization over 1850-2100 (n = 251 model years). This procedure yields a spatially varying distribution of parameters that accounts for both model structural uncertainty and internal climate variability. Because each GCM has a different number of ensemble members (Table A1), medians across models are weighted by the inverse of the number of ensemble members per GCM, so that each GCM has equal weight.

The main analysis treats each parameter as linear in cumulative emissions, motivated by the existing evidence for linear proportionality between emissions and the magnitude of local

heat and rainfall extremes (Seneviratne et al., 2016). It is important to note, however, that even linear shifts in the location of a distribution can lead to nonlinear changes in the frequency of extreme events in the tail of that distribution, so nonlinearity in extreme event risk is still permitted by the main specification (Patel et al., 2024).

2.3 Comparing parameters to observations

To test whether the GCM-derived parameters are realistic, they are compared to distributions of the same parameters derived using observed TXx and Rx1day data and observed emissions. Because trends in local climate extremes can be strongly influenced by internal climate variability (Fischer et al., 2013), the most appropriate test is whether the observational parameters fall within the distribution of parameters derived from GCMs. Specifically, if the observed parameter falls within the 99% range of the ensemble for each parameter at each grid cell, the observations can be considered consistent with the GCM-derived paramters. Slope parameters for both location and scale (β_1 and θ_1) are required to fall within the GCM-derived distributions at each grid cell; if either does not, that grid cell is excluded from the analysis. Because the observational parameters are only fit using data from 1979-2024, this comparison uses parameters fit to model years 1979-2024 in each GCM rather than the full time period.

2.4 Assessing GEV goodness-of-fit

It is important to assess whether the GEV is an appropriate distribution for representing the underlying GCM data. To do so, each GCM realization is compared to an idealized GEV distribution (Risser, Zhang, et al., 2025). Each GCM realization is normalized by subtracting the corresponding estimated GEV location and dividing by the scale, which yields a time series with location 0, scale 1, and shape ζ. A synthetic GEV distribution is then generated, similarly with location 0, scale 1, and shape ζ. Finally, a Kolmogorov-Smirnov (K-S) test is performed to assess whether these two distributions were drawn from the same underlying distribution. The null hypothesis for this test is that the two distributions are indistinguishable; if the null hypothesis is rejected, the GEV distribution is considered a poor fit to the data. This test is performed separately for each of 171 GCM realizations at each grid cell.

This procedure also provides information on whether a linear fit is appropriate for the data. If the underlying data are linear, normalizing by linear coefficients will yield a normalized GEV time series that is very similar to the idealized GEV distribution. However, if the underlying data are nonlinear, normalizing by linear coefficients will still leave residual variation in the data that is not included in the idealized GEV, thus leading to a mismatch that fails the K-S test. Fig. S3 provides an example of this procedure using simulated data.

This approach raises a multiple-testing issue: performing many statistical tests across many grid cells is likely to cause false rejections of the null in some locations (Wilks, 2016). However, in the case of this study, this tendency makes the analysis conservative: guarding against false rejections would raise the threshold for concluding that the GCM data and GEV distribution are mismatched, and would make it even more likely to conclude that the two distributions cannot be distinguished.

2.5 Attributing extreme event risk to individual actors

The framework used in this paper yields estimates of how the parameters of extreme event distributions change with cumulative emissions. To attribute extreme event risk to individual emitters, the probability of a particular extreme event is calculated twice: once based on the parameters evaluated for all historical emissions at the time of the extreme event, and again based on the parameters evaluated with the emissions of a particular actor removed (Fig. 1). The ratio of these "factual" and "counterfactual" probabilities is the change in probability due to the emissions of that actor.

3 Results

Extreme heat and rainfall broadly increase with cumulative CO_2 emissions across the globe (Fig. 2). The magnitude of the average annual hottest day (indicated by the location of the TXx distribution) universally increases with CO_2 emissions across land grid cells between 65 °S and 65 °N (Fig. 2a). However, there is little consistent change in year-to-year variability (indicated by the scale parameter; Fig. 2b), suggesting that changes in extreme heat are driven by overall shifts in the distribution of annual maxima and not changes in variability. Changes in Rx1day are more spatially heterogeneous, but the magnitude and variability of the Rx1day distribution both increase with cumulative CO_2 emissions across >70% of grid cells (Fig. 2c, 2d).

Two tests can assess whether these fitted parameters represent a skillful and appropriate fit to the underlying data. First, the GCM-derived parameters are compared to the same parameters fitted to observations (Fig. S4) to assess whether the models are skillful. If either the location shift or scale shift parameters from observations falls outside the GCM distribution at a given grid cell, the grid cell is excluded from the analysis (Fig. S5). This procedure excludes 3% of grid cells for TXx and 26% of grid cells for Rx1day (Fig. 2, Fig. S5).

Second, the GEV goodness-of-fit can be assessed by normalizing each GCM realization and comparing it to an idealized GEV distribution (Methods). Across grid cells and GCMs, there is no consistent evidence that the GCM simulations differ from a theoretical GEV distribution. At each grid cell, ~5% of statistical tests should yield *p*-values below 0.05 even if the null hypothesis were true; across 97% of land grid cells, less than 5% of *p*-values are below 0.05 for both TXx and Rx1day, suggesting a broad inability to reject the null hypothesis that the GCM data are drawn from a GEV distribution (Fig. S6). The region where the most significant mismatch is apparent is in the Sahara Desert for Rx1day (Fig. S6), a region where there is not observe a strong effect of emissions on extreme rainfall risk (Fig. 2), so a potential mismatch in this area should not strongly affect the overall analysis. Importantly, this result suggests that despite the expectation of nonlinear increases in extreme rainfall intensity with warming, a GEV fit that allows parameters to shift linearly with cumulative emissions still provides a reliable representation of the data.

With confidence in the framework, CO_2 emissions can be directly related to the probability of the most extreme daily heat or rainfall at each grid cell in the last five years (since 2020). The focus here is on several emitters whose cumulative CO_2 emissions have altered the probability of these events: the United States, ExxonMobil, and an arbitrary actor responsible for 20 $GtCO_2$ (to illustrate the flexibility of the approach) (Fig. 3). Given the monotonic relationship between emissions and extreme heat, each actor has contributed to increases in extreme heat probability across all non-missing land grid cells (Fig. 3a-c). The United States, emitting 390

$GtCO_2$ before 2020, has doubled the probability of post-2020 extreme heat events for 10% of grid cells. ExxonMobil has had a smaller effect due to its smaller emissions (48 $GtCO_2$), but is still responsible for increases in extreme event probability of at least 5% in one-third of the grid cells analyzed. The effect of these actors is smaller in magnitude for rainfall than for temperature, but consistent increases in extreme rainfall risk are apparent across global land areas (Fig. 3d-f). These actors are merely chosen to be illustrations of the application of the method, and the approach could be applied to any actor whose cumulative emissions are known over some timeframe.

The main analysis models GEV parameters as linear functions of the covariates (Methods). While even linear distribution shifts can lead to nonlinear increases in the frequency of extreme events (Patel et al., 2024), it may also be appropriate to model the individual parameters nonlinearly. Figure S7 shows probability ratios for the effect of ExxonMobil's emissions on TXx and Rx1day (i.e., analogous to Fig. 3b, 3e) when the location and scale parameters are fitted with a quadratic function, or when the scale parameter is fitted with an exponential function (Risser & Wehner, 2017). In both cases, estimated changes in extreme event probability across the globe are similar to results from the linear model ($R^2 >= 0.94$), suggesting that a linear model is broadly sufficient to account for changes in heat and rainfall risk due to cumulative emissions.

An alternative approach to nonlinearity is to estimate GEV parameters over subsections of the overall time period, which is illustrated for a single realization and grid cell in Fig. S8. However, given the strong influence of internal variability on decadal timescales (Hawkins & Sutton, 2009), the above tests are more systematic assessments of nonlinearity in the forced response of extreme events to cumulative emissions.

The framework can also be applied to specific TXx or Rx1day events that have been the subject of recent litigation, such as the 2021 heat wave in the Pacific Northwest or 2022 rainfall in Pakistan (Fig. 4). By comparing estimates of the probabilities of these events with and without specific emissions contributions (Fig. 4a, 4c), the effects of those contributions on the event risk can be quantified (Fig. 4b, 4d). The central estimate is that the ten highest-emitting privately owned carbon majors increased the risk of extreme heat in the Pacific Northwest by 1.31—i.e., that the 2021 Pacific Northwest heat wave was 31% more likely due to their emissions. These carbon majors have also made the risk of extreme rainfall in Pakistan around 7% more likely (Fig. 4b).

Uncertainty in these probability changes arises from the differing parameter estimates across the 171 MMLEA realizations, which is due to both differences in model structure and initial-condition uncertainty across multiple realizations of a single model. The shading in Fig. 4b and 4d correspond to the inner 66% and 90% ranges across this ensemble of 171 parameters, based on the IPCC "likely" and "very likely" ranges (Mastrandrea et al., 2010). Uncertainty is notably lower for heat than rainfall, with a 90% range of 1.17 – 1.46 for the carbon majors' contribution to the 2021 Pacific Northwest heat wave and 1.001 – 1.23 for their contribution to the 2022 rainfall in Pakistan.

4 Discussion

These findings inform both legal and political applications of climate liability. In the legal context where private fossil fuel producers are typically the target, such as civil lawsuits in

the U.S., standing for plaintiffs depends on demonstrating a causal chain between an emitter and a climate impact. This study clarifies these causal chains by showing a direct proportionality between emissions and the rising risk of extreme heat and rainfall. In the political context where major countries are typically the target, such as allocation of international financial payments for loss and damage, a consistent framework for end-to-end attribution can inform the allocation of funds alongside standard extreme event attribution approaches (Noy et al., 2023).

The flexibility of this framework means that the fitted parameters can be applied to any actor whose CO_2 emissions are known over some time period, without the need to re-estimate the relationship between emissions and extreme temperature and rainfall. This approach is conceptually similar to "pre-computed" approaches to extreme event attribution, in which the relationship between climate change and extreme events is estimated first and then applied to new events as desired (Christidis et al., 2015). Accordingly, it is worth emphasizing that the choice of actors (the U.S., ExxonMobil, etc.) is purely illustrative of the potential application of the framework, and could be replaced by any other actor of interest. This advantage contrasts with some other recent end-to-end attribution approaches using reduced-complexity climate models, which require re-running the model and re-estimating counterfactual scenarios each time a new actor is incorporated into the framework (Callahan & Mankin, 2025; Quilcaille et al., 2025).

These findings additionally lend support to the principle that "every ton matters." Policymakers have sometimes argued that any individual actor's emissions are so minimal as to be irrelevant to climate risk, in both legal cases such as *Held v. Montana* and policies such as the U.S. EPA's 2025 proposed repeal of the 2009 Endangerment Finding. By quantitatively demonstrating that local extreme event probabilities are proportional to CO_2 emissions, this study shows that emitters cannot escape responsibility for climate impacts by claiming that those impacts are too diffuse or complex to be attributed to fossil fuels.

One drawback of the framework is that the proportional relationships between cumulative emissions, global warming, and extremes apply only to CO_2, since it is a long-lived pollutant. Shorter-lived GHGs like methane also have substantial radiative forcing effects, and aerosols have spatially heterogeneous cooling effects not captured by global proportional relationships. However, to first order, the IPCC assessed the effective radiative forcing of non-CO_2 GHGs and aerosols to be similar in magnitude with opposite signs (Forster et al., 2021), suggesting that incorporating both of these influences would only slightly alter the results on a global scale. That said, incorporation of short-lived climate pollutants and aerosols into end-to-end attribution frameworks is not simple and deserves additional focus as the field progresses.

Additionally, caution is warranted when applying this framework to other climate impacts—either physical hazards such as flooding or drought, or downstream human impacts such as heat-related mortality—for two reasons. First, these other impacts may exhibit nonlinear responses to forcing, such as a levee overtopping during a flood or a rapid increase in mortality above a critical temperature. Such nonlinearities are not easily captured in this approach and should be explicitly assessed in future work. Second, the framework presented here is focused on the probability of extreme events and not their magnitude. The human impacts of extreme events generally depend on magnitude rather than probability, so GEV-based estimates of changing probability should not be directly applied to downstream impact estimates (Callahan et al., 2025; Perkins-Kirkpatrick et al., 2022).

This study uses observational datasets with global coverage to provide an assessment of the effects of cumulative emissions on a broad range of recent extreme events. However, this strategy does not account for observational uncertainty, and these global datasets may perform less effectively in any particular region. The GEV parameters are fitted to climate models rather than observations precisely to reduce the influence of this uncertainty on the estimates, but it remains a consideration when estimating the magnitudes of extreme events upon which attribution is performed. Future work that takes advantage of regional observing stations or regional reanalyses may better capture the magnitude of extreme events that are of interest to local stakeholders. Additionally, the broad inequity in global weather observations (Su et al., 2026) and disaster databases (Harrington & Otto, 2020) means that enhancing broader observational capacity in lower-income regions will be essential to making attribution accessible to vulnerable populations in the future.

5 Conclusion

This study demonstrates a framework for end-to-end climate attribution that leverages proportional relationships between cumulative CO_2 emissions and the changing risk of extreme climate events. This approach provides flexible, rapid assessments of how individual actors have contributed to climate risk globally and specific events in particular. Most importantly, this approach demonstrates that each ton of CO_2 emitted raises the likelihood of extreme climate impacts. Given that these impacts have already been accelerated by greenhouse gas emissions, rapid emissions reductions will be necessary to avoid further amplification of climate risk.

Acknowledgments

I thank M.D. Risser for feedback on the analysis and interpretation of results. Some of this research was performed using Indiana University high-performance computing systems, which were supported in part by Lilly Endowment, Inc., through its support for the Indiana University Pervasive Technology Institute.

Open Research

All data and code used for the analysis are publicly available. The Multi-Model Large Ensemble Archive is available at: https://www.cesm.ucar.edu/community-projects/mmlea. Global Carbon Budget data are available at: https://globalcarbonbudget.org/. The Carbon Majors database is available at: https://carbonmajors.org. CEDS data are available at: https://github.com/JGCRI/CEDS. ERA5 data are available at: https://cds.climate.copernicus.eu/datasets/reanalysis-era5-single-levels. CPC data are available at: https://psl.noaa.gov/data/gridded/data.cpc.globalprecip.html. The computer code used for the analysis is publicly available at: https://github.com/ccallahan45/Cumulative_Emissions_Attribution.

Conflict of Interest Disclosure

The author declares there are no conflicts of interest for this manuscript.

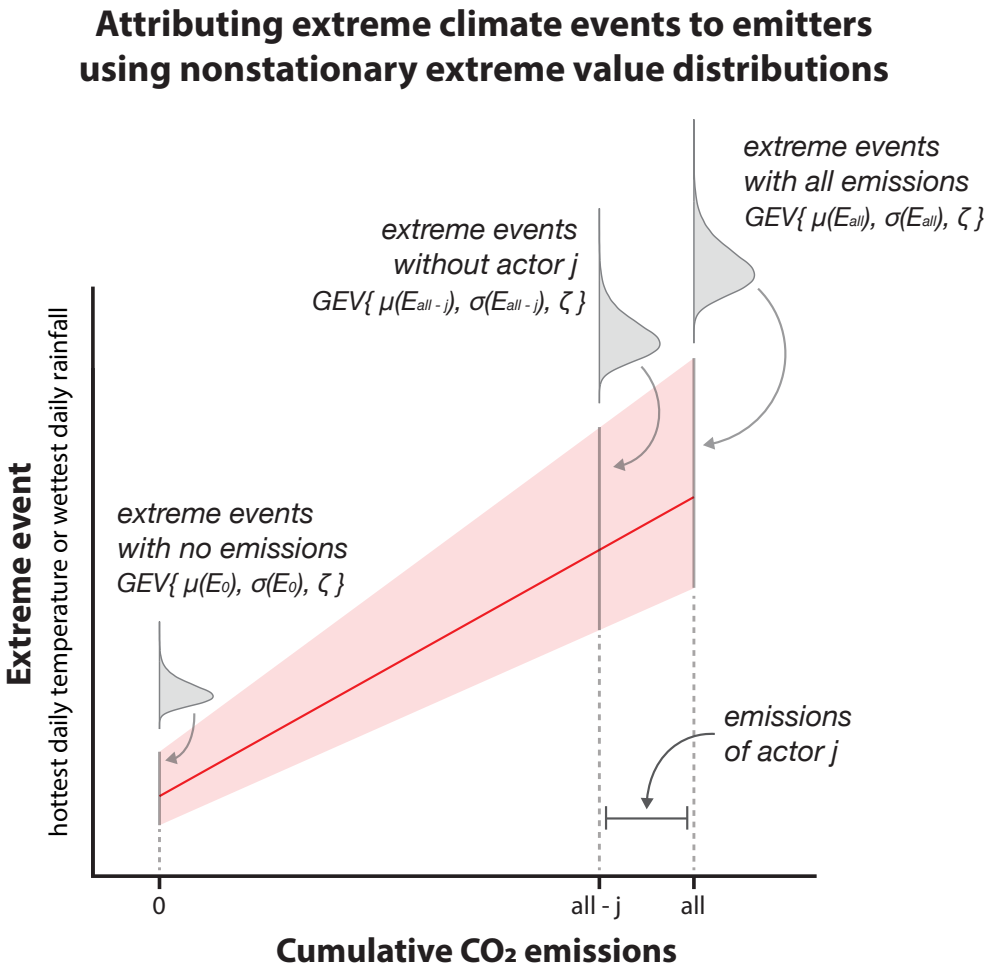

Figure 1: Schematic of analysis. Using ensembles of climate model simulations, nonstationary GEVs are fit that allow the location and scale parameters to vary as a function of cumulative CO_2 emissions at each grid cell. The probability of extreme events can then be predicted at some given level of cumulative emissions. To assess the contribution of an individual emitter, the cumulative emissions of that actor can be subtracted from total emissions and the change in extreme event risk can be quantified.

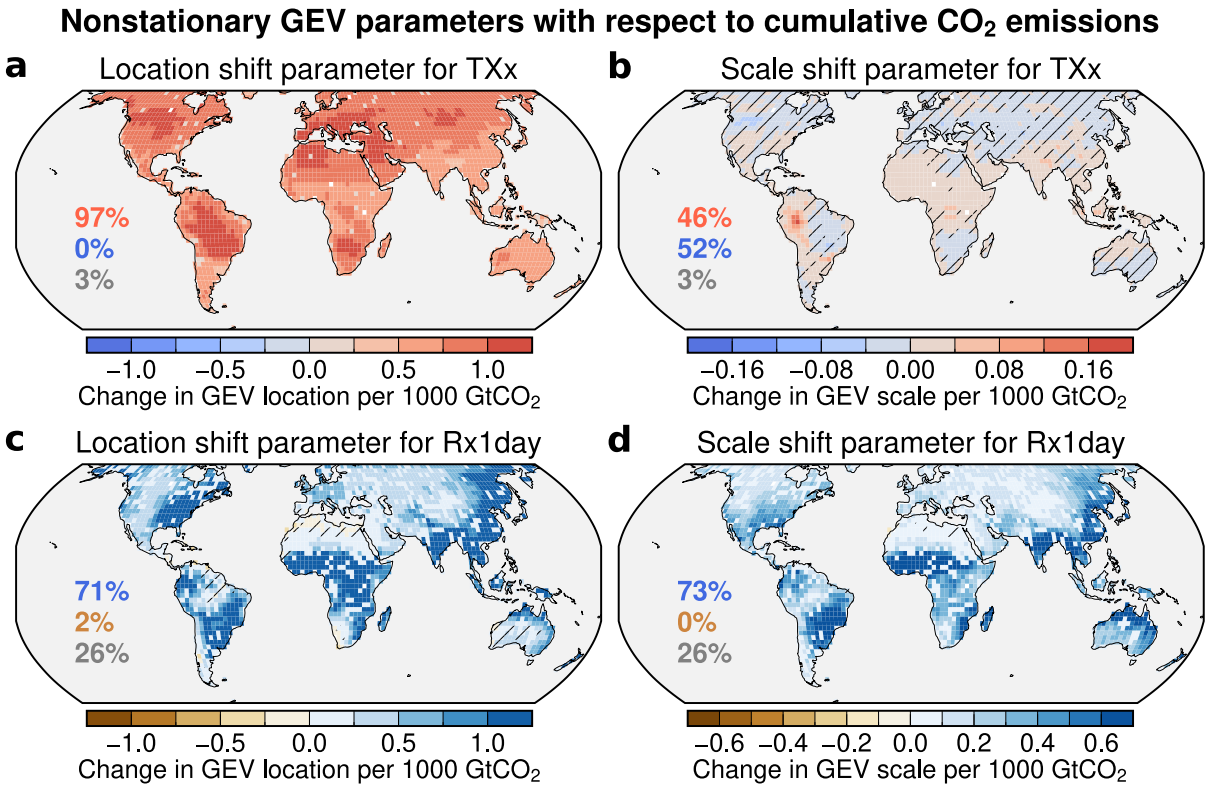

Figure 2: Fitted GEV parameters. a) Change in GEV location for TXx (hottest day of the year) as a function of cumulative CO_2 emissions. b) Change in GEV scale for TXx as a function of cumulative emissions. c) As in (a), but for Rx1day (wettest day of the year). d) As in (b), but for Rx1day. Each map shows the weighted median across parameters estimated from separate GCM realizations. Grid cells are not colored if the observational parameters fall outside the model ensemble and are hatched if less than 66% of GCM realizations agree on the sign of the parameter. Inset text denotes the percent of land grid cells over 65 °S – 65 °N with positive or negative parameter values, and the percent of grid cells that are dropped in gray (Methods).

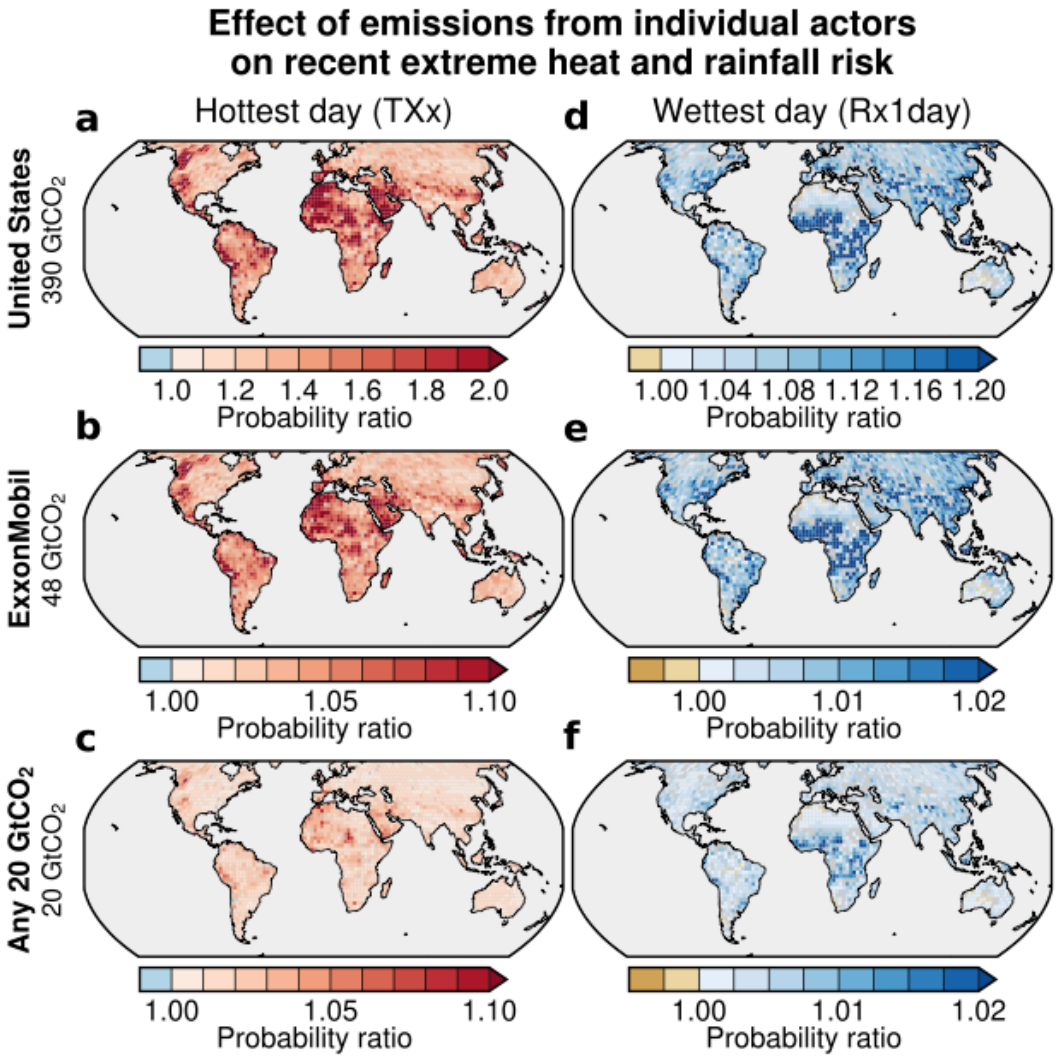

Figure 3: Recent extreme heat and rainfall events attributed to individual emitters. Each map shows the change in probability of the most extreme heat (a-c) or rainfall (d-f) event since 2020, due to cumulative CO_2 emissions from the United States (a, d), ExxonMobil (b, e), and an arbitrary actor contributing 20 $GtCO_2$ (c, f). Probability changes are expressed as ratios; for example, a ratio of 1.1 denotes a 10% increase in probability. Grid cells are colored gray if the observational parameters fall outside the model ensemble (Methods). Note that the color bar ranges are different for different subplots.

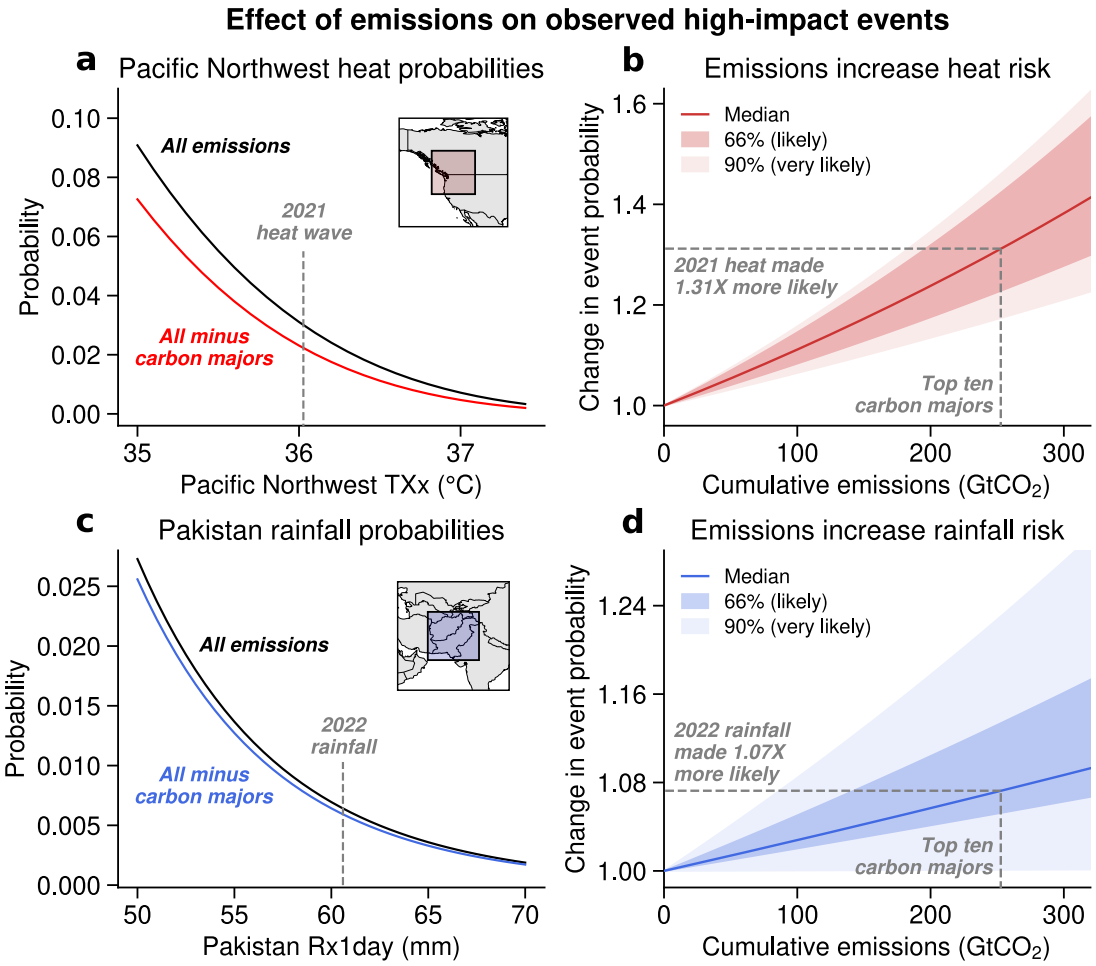

Figure 4: Cumulative emissions have increased the risk of high-profile events. Panels (a) and (c) show the ensemble median probabilities of TXx values in the Pacific Northwest (a) and Rx1day values in Pakistan (c). Black lines denote factual scenarios with all emissions and red or blue lines denote counterfactual scenarios in which the emissions of the top ten privately owned fossil fuel producers ("carbon majors") have been subtracted. Dashed gray line denotes the observed magnitude of the specific event of interest. Inset maps show the boundaries for each selected region: 230-250 °E, 40-60 °N for the Pacific Northwest and 60-77 °E, 23-39 °N for Pakistan. Panels (b) and (d) show the change in probability of each event across a range of emissions, calculated as the ratio of the factual probability to the counterfactual probability. Solid line shows median, light shading shows 90% range (IPCC "very likely" range) across the parameter ensemble, and darker shading shows 66% range (IPCC "likely" range). Dashed line denotes the median effect of the top ten carbon majors. In all panels, top ten carbon majors are Chevron, ExxonMobil, Shell, BP, ConocoPhillips, Total, Peabody, Occidental, BHP, and CONSOL.

References

Allen, M. (2003). Liability for climate change. *Nature*, *421*(6926), 891–892.

Beusch, L., Nauels, A., Gudmundsson, L., Gütschow, J., Schleussner, C.-F., & Seneviratne, S. I. (2022). Responsibility of major emitters for country-level warming and extreme hot years. *Communications Earth & Environment*, *3*(1), 1–7. https://doi.org/10.1038/s43247-021-00320-6

Burger, M., Wentz, J., & Horton, R. (2020). The law and science of climate change attribution. *Colum. J. Envtl. L.*, *45*, 57.

Burke, M., Zahid, M., Diffenbaugh, N. S., & Hsiang, S. (2026). Quantifying climate loss and damage consistent with a social cost of carbon. *Nature*, *651*(8107), 959–966. https://doi.org/10.1038/s41586-026-10272-6

Calhoun, M., Rothschild, R., Binder, J., Mihaly, E., Mankin, J., Lippard, B., & Wood, M. (2025). Examining State Climate Superfund Legislation. *Environmental Law Reporter*, *55*(3), 10251–10262.

Callahan, C. W., & Mankin, J. S. (2022). National attribution of historical climate damages. *Climatic Change*, *172*(3), 40. https://doi.org/10.1007/s10584-022-03387-y

Callahan, C. W., & Mankin, J. S. (2025). Carbon majors and the scientific case for climate liability. *Nature*, *640*(8060), 893–901. https://doi.org/10.1038/s41586-025-08751-3

Callahan, C. W., Trok, J. T., Wilson, A. J., Gould, C. F., Heft-Neal, S., Burke, M., & Diffenbaugh, N. S. (2025). Quantifying the contributions of climate change and adaptation to mortality from unprecedented extreme heat events. *Proceedings of the National Academy of Sciences*, *122*(51), e2503577122. https://doi.org/10.1073/pnas.2503577122

Christidis, N., Stott, P. A., & Zwiers, F. W. (2015). Fast-track attribution assessments based on pre-computed estimates of changes in the odds of warm extremes. *Climate Dynamics*, *45*(5), 1547–1564. https://doi.org/10.1007/s00382-014-2408-x

Clarke, R. H., Wescombe, N. J., Huq, S., Khan, M., Kramer, B., & Lombardi, D. (2023). Climate loss-and-damage funding: A mechanism to make it work. *Nature*, *623*(7988), 689–692. https://doi.org/10.1038/d41586-023-03578-2

Coles, S. (2001). *An Introduction to Statistical Modeling of Extreme Values*.

Dahl, K. A., Abatzoglou, J. T., Phillips, C. A., Ortiz-Partida, J. P., Licker, R., Merner, L. D., & Ekwurzel, B. (2023). Quantifying the contribution of major carbon producers to increases in vapor pressure deficit and burned area in western US and southwestern Canadian forests. *Environmental Research Letters*, *18*(6), 064011. https://doi.org/10.1088/1748-9326/acbce8

Deser, C., Lehner, F., Rodgers, K. B., Ault, T., Delworth, T. L., DiNezio, P. N., Fiore, A., Frankignoul, C., Fyfe, J. C., Horton, D. E., Kay, J. E., Knutti, R., Lovenduski, N. S., Marotzke, J., McKinnon, K. A., Minobe, S., Randerson, J., Screen, J. A., Simpson, I. R., & Ting, M. (2020). Insights from Earth system model initial-condition large ensembles and future prospects. *Nature Climate Change*, *10*(4), 277–286. https://doi.org/10.1038/s41558-020-0731-2

Diffenbaugh, N. S., Singh, D., Mankin, J. S., Horton, D. E., Swain, D. L., Touma, D., Charland, A., Liu, Y., Haugen, M., Tsiang, M., & others. (2017). Quantifying the influence of global warming on unprecedented extreme climate events. *Proceedings of the National Academy of Sciences*, *114*(19), 4881–4886.

Ekwurzel, B., Boneham, J., Dalton, M. W., Heede, R., Mera, R. J., Allen, M. R., & Frumhoff, P. C. (2017). The rise in global atmospheric CO2, surface temperature, and sea level from emissions traced to major carbon producers. *Climatic Change*, *144*(4), 579–590. https://doi.org/10.1007/s10584-017-1978-0

Fischer, E. M., Beyerle, U., & Knutti, R. (2013). Robust spatially aggregated projections of climate extremes. *Nature Climate Change*, *3*(12), 1033–1038. https://doi.org/10.1038/nclimate2051

Fischer, E. M., & Knutti, R. (2015). Anthropogenic contribution to global occurrence of heavy-precipitation and high-temperature extremes. *Nature Climate Change*, *5*(6), 560–564. https://doi.org/10.1038/nclimate2617

Forster, P., Storelvmo, T., Armour, K., Collins, W., Dufresne, J.-L., Frame, D., Lunt, D. J., Mauritsen, T., Palmer, M. D., Watanabe, M., Wild, M., & Zhang, H. (2021). The Earth's Energy Budget, Climate Feedbacks, and Climate Sensitivity. In *Climate Change 2021: The Physical Science Basis. Contribution of Working Group I to the Sixth Assessment Report of the Intergovernmental Panel on Climate Change* (pp. 923–1054).

Friedlingstein, P., O'Sullivan, M., Jones, M. W., Andrew, R. M., Hauck, J., Landschützer, P., Le Quéré, C., Li, H., Luijkx, I. T., Olsen, A., Peters, G. P., Peters, W., Pongratz, J., Schwingshackl, C., Sitch, S., Canadell, J. G., Ciais, P., Jackson, R. B., Alin, S. R., … Zeng, J. (2025). Global Carbon Budget 2024. *Earth System Science Data*, *17*(3), 965–1039. https://doi.org/10.5194/essd-17-965-2025

Gilleland, E., & Katz, R. W. (2016). extRemes 2.0: An Extreme Value Analysis Package in R. *Journal of Statistical Software*, *72*, 1–39. https://doi.org/10.18637/jss.v072.i08

Harrington, L. J., & Otto, F. E. (2020). Reconciling theory with the reality of African heatwaves. *Nature Climate Change*, *10*(9), 796–798.

Hawkins, E., & Sutton, R. (2009). The potential to narrow uncertainty in regional climate predictions. *Bulletin of the American Meteorological Society*, *90*(8), 1095–1108.

Heede, R. (2014). Tracing anthropogenic carbon dioxide and methane emissions to fossil fuel and cement producers, 1854–2010. *Climatic Change*, *122*(1), 229–241. https://doi.org/10.1007/s10584-013-0986-y

Hersbach, H., Bell, B., Berrisford, P., Hirahara, S., Horányi, A., Muñoz-Sabater, J., Nicolas, J., Peubey, C., Radu, R., Schepers, D., Simmons, A., Soci, C., Abdalla, S., Abellan, X., Balsamo, G., Bechtold, P., Biavati, G., Bidlot, J., Bonavita, M., … Thépaut, J.-N. (2020). The ERA5 global reanalysis. *Quarterly Journal of the Royal Meteorological Society*, *146*(730), 1999–2049. https://doi.org/10.1002/qj.3803

Hoesly, R. M., Smith, S. J., Feng, L., Klimont, Z., Janssens-Maenhout, G., Pitkanen, T., Seibert, J. J., Vu, L., Andres, R. J., Bolt, R. M., & others. (2018). Historical (1750-2014) anthropogenic emissions of reactive gases and aerosols from the Community Emission Data System (CEDS). *Geoscientific Model Development*, *11*, 369–408.

IPCC. (2021). Summary for Policymakers. In V. Masson-Delmotte, P. Zhai, A. Pirani, S. L. Connors, C. Péan, S. Berger, N. Caud, Y. Chen, L. Goldfarb, M. I. Gomis, M. Huang, K. Leitzell, E. Lonnoy, J. B. R. Matthews, T. K. Maycock, T. Waterfield, O. Yelekçi, R. Yu, & B. Zhou (Eds.), *Climate Change 2021: The Physical Science Basis. Contribution of Working Group I to the Sixth Assessment Report of the Intergovernmental Panel on Climate Change*. Cambridge University Press. https://www.ipcc.ch/report/ar6/wg1/downloads/report/IPCC_AR6_WGI_SPM.pdf

Kysar, D. A. (2011). What Climate Change Can Do About Tort Law. *Environmental Law*, *41*(1), 1–71.

Lott, F. C., Ciavarella, A., Kennedy, J. J., King, A. D., Stott, P. A., Tett, S. F. B., & Wang, D. (2021). Quantifying the contribution of an individual to making extreme weather events more likely. *Environmental Research Letters*, *16*(10), 104040. https://doi.org/10.1088/1748-9326/abe9e9

Maher, N., Phillips, A. S., Deser, C., Wills, R. C. J., Lehner, F., Fasullo, J., Caron, J. M., Brunner, L., Beyerle, U., & Jeffree, J. (2025). The updated Multi-Model Large Ensemble Archive and the Climate Variability Diagnostics Package: New tools for the study of climate variability and change. *Geoscientific Model Development*, *18*(18), 6341–6365. https://doi.org/10.5194/gmd-18-6341-2025

Mastrandrea, M. D., Field, C.B., Stocker, T.F., Edenhofer, O., Ebi, K.L., Frame, D.J., Held, H., Kriegler, E., Mach, K.J., Matschoss, P.R., Plattner, G.-K., Yohe, G.W., & Zwiers, F.W. (2010). *Guidance Note for Lead Authors of the IPCC Fifth Assessment Report on Consistent Treatment of Uncertainties*. Intergovernmental Panel on Climate Change (IPCC).

Matthews, H. D., & Caldeira, K. (2008). Stabilizing climate requires near-zero emissions. *Geophysical Research Letters*, *35*(4). https://doi.org/10.1029/2007GL032388

Matthews, H. D., Gillett, N. P., Stott, P. A., & Zickfeld, K. (2009). The proportionality of global warming to cumulative carbon emissions. *Nature*, *459*(7248), 829.

Meehl, G. A., Senior, C. A., Eyring, V., Flato, G., Lamarque, J.-F., Stouffer, R. J., Taylor, K. E., & Schlund, M. (2020). Context for interpreting equilibrium climate sensitivity and transient climate response from the CMIP6 Earth system models. *Science Advances*, *6*(26), eaba1981.

Miralles, O., & Davison, A. C. (2023). Timing and spatial selection bias in rapid extreme event attribution. *Weather and Climate Extremes*, *41*, 100584. https://doi.org/10.1016/j.wace.2023.100584

Noy, I., Wehner, M., Stone, D., Rosier, S., Frame, D., Lawal, K. A., & Newman, R. (2023). Event attribution is ready to inform loss and damage negotiations. *Nature Climate Change*, *13*(12), 1279–1281. https://doi.org/10.1038/s41558-023-01865-4

Otto, F. E. L., Skeie, R. B., Fuglestvedt, J. S., Berntsen, T., & Allen, M. R. (2017). Assigning historic responsibility for extreme weather events. *Nature Climate Change*, *7*(11), 757.

Patel, R. N., Bonan, D. B., & Schneider, T. (2024). Changes in the Frequency of Observed Temperature Extremes Largely Driven by a Distribution Shift. *Geophysical Research Letters*, *51*(24), e2024GL110707. https://doi.org/10.1029/2024GL110707

Perkins-Kirkpatrick, S. E., Stone, D. A., Mitchell, D. M., Rosier, S., King, A. D., Lo, Y. T. E., Pastor-Paz, J., Frame, D., & Wehner, M. (2022). On the attribution of the impacts of extreme weather events to anthropogenic climate change. *Environmental Research Letters*, *17*(2), 024009. https://doi.org/10.1088/1748-9326/ac44c8

Phelan, A. L., Meier, B. M., Patterson, D. W., Hesselman, M., Tahzib, F., & Gostin, L. O. (2025). The ICJ Advisory Opinion: A legal mandate for planetary health. *The Lancet*, *406*(10508), 1068–1070. https://doi.org/10.1016/S0140-6736(25)01725-8

Philip, S., Kew, S., van Oldenborgh, G. J., Otto, F., Vautard, R., van der Wiel, K., King, A., Lott, F., Arrighi, J., Singh, R., & van Aalst, M. (2020). A protocol for probabilistic extreme event attribution analyses. *Advances in Statistical Climatology, Meteorology and Oceanography*, *6*(2), 177–203. https://doi.org/10.5194/ascmo-6-177-2020

Quilcaille, Y., Gudmundsson, L., Schumacher, D. L., Gasser, T., Heede, R., Heri, C., Lejeune, Q., Nath, S., Naveau, P., Thiery, W., Schleussner, C.-F., & Seneviratne, S. I. (2025). Systematic attribution of heatwaves to the emissions of carbon majors. *Nature*, *645*(8080), 392–398. https://doi.org/10.1038/s41586-025-09450-9

Risser, M. D., Ombadi, M., & Wehner, M. F. (2025). Granger causal inference for climate change attribution. *Environmental Research: Climate*, *4*(2), 022001. https://doi.org/10.1088/2752-5295/add046

Risser, M. D., & Wehner, M. F. (2017). Attributable human-induced changes in the likelihood and magnitude of the observed extreme precipitation during Hurricane Harvey. *Geophysical Research Letters*, *44*(24), 12–457.

Risser, M. D., Zhang, L., & Wehner, M. F. (2025). Data-driven upper bounds and event attribution for unprecedented heatwaves. *Weather and Climate Extremes*, *47*, 100743. https://doi.org/10.1016/j.wace.2025.100743

Saad, A. I. (2023). Attribution for Climate Torts. *Boston College Law Review*, *64*(4). https://bclawreview.bc.edu/articles/3073

Sadai, S., Ranganathan, M., Nauels, A., Nicholls, Z., Merner, D., Dahl, K., Licker, R., & Ekwurzel, B. (2025). Estimating the sea level rise responsibility of industrial carbon producers. *Environmental Research Letters*, *20*(4), 044012. https://doi.org/10.1088/1748-9326/adb59f

Schöngart, S., Nicholls, Z., Hoffmann, R., Pelz, S., & Schleussner, C.-F. (2025). High-income groups disproportionately contribute to climate extremes worldwide. *Nature Climate Change*, *15*(6), 627–633. https://doi.org/10.1038/s41558-025-02325-x

Seneviratne, S. I., Donat, M. G., Pitman, A. J., Knutti, R., & Wilby, R. L. (2016). Allowable CO2 emissions based on regional and impact-related climate targets. *Nature*, *529*(7587), 477–483.

Setzer, J., & Higham, C. (2024). *Global trends in climate change litigation: 2024 snapshot*. Grantham Research Institute on Climate Change and the Environment and Centre for Climate Change Economics and Policy, London School of Economics and Political Science.

Su, J., Miao, C., Zwiers, F., Beck, H., Jones, P., Sun, Q., Slater, L. J., Berghuijs, W. R., Wada, Y., Rosenfeld, D., Gou, J., Wu, Y., Tarolli, P., Borrelli, P., Panagos, P., Alexander, L. V., Zhang, Q., Hu, J., Min, S.-K., … Sorooshian, S. (2026). Precipitation observing network gaps limit climate change impact assessment. *Nature*, *652*(8108), 119–125. https://doi.org/10.1038/s41586-026-10300-5

Trok, J. T., Barnes, E. A., Davenport, F. V., & Diffenbaugh, N. S. (2024). Machine learning–based extreme event attribution. *Science Advances*, *10*(34), eadl3242. https://doi.org/10.1126/sciadv.adl3242

van Oldenborgh, G. J., van der Wiel, K., Kew, S., Philip, S., Otto, F., Vautard, R., King, A., Lott, F., Arrighi, J., Singh, R., & van Aalst, M. (2021). Pathways and pitfalls in extreme event attribution. *Climatic Change*, *166*(1), 13. https://doi.org/10.1007/s10584-021-03071-7

Wilks, D. S. (2016). *"The Stippling Shows Statistically Significant Grid Points": How Research Results are Routinely Overstated and Overinterpreted, and What to Do about It*. https://doi.org/10.1175/BAMS-D-15-00267.1

Xie, P., Chen, M., & Shi, W. (2010). CPC unified gauge-based analysis of global daily precipitation. *Preprints, 24th Conf. on Hydrology, Atlanta, GA, Amer. Meteor. Soc*, *2*.

Zeder, J., Sippel, S., Pasche, O. C., Engelke, S., & Fischer, E. M. (2023). The Effect of a Short Observational Record on the Statistics of Temperature Extremes. *Geophysical Research Letters*, *50*(16), e2023GL104090. https://doi.org/10.1029/2023GL104090